J. Fluid Mech. (2009), *vol.* 622, *pp.* 195–207. © 2009 Cambridge University Press
doi:10.1017/S0022112008005193 Printed in the United Kingdom

Boundary effects on electro-magneto-phoresis

EHUD YARIV[1]† AND TOUVIA MILOH[2]

[1]Faculty of Mathematics, Technion – Israel Institute of Technology, Technion City 32000, Israel
[2]School of Mechanical Engineering, Faculty of Engineering, Tel Aviv University, Ramat Aviv 69978, Israel

(Received 14 July 2008 and in revised form 26 October 2008)

The effect of a remote insulating boundary on the electro-magneto-phoretic motion of an insulating spherical particle suspended in a conducting liquid is investigated using an iterative reflection scheme developed about the unbounded-fluid-domain solution of Leenov & Kolin (*J. Chem. Phys.*, vol. 22, no. 4, p. 683). Wall-induced corrections result from velocity reflections, successively introduced so as to maintain the no-slip condition on the wall and particle boundaries, as well as from the Lorentz forces associated with comparable reflections of the electric field. This method generates asymptotic expansions in λ ($\ll 1$), the ratio of particle size to particle–wall separation. The leading-order correction to the hydrodynamic force on the particle appears at $O(\lambda^3)$; it is directed along the leading-order force and tends to augment it.

1. Introduction

When uniform electric and magnetic fields are externally applied in an electrically conducting liquid, a uniform Lorentz force density is generated. In a bounded domain, this body force is balanced by a hydrostatic-like pressure distribution, and the liquid remains at rest. If an insulating particle (say of matching magnetic permeability) is introduced into the liquid, it experiences a force whose source is twofold: an 'electromagnetic buoyancy', arising from that distribution, and a viscous-flow contribution, generated by the rotational Lorentz force density associated with the expulsion of current lines from the volume occupied by the particle. The ensuing motion of a freely suspended particle, known as 'electro-magneto-phoresis', is employed in various biological (Kolin & Kado 1958; Kolin 1978; Watarai, Suwa & Iiguni 2004) and metallurgical (Xu, Li & Zhou 2007) applications.

The pioneering theoretical analysis of this phenomenon was carried out by Leenov & Kolin (1954) who calculated the flow about a spherical particle which is suspended in an unbounded fluid domain. The strive to understand the response of more complicated particle geometries has led to the development of general symmetry analysis for arbitrary body shapes (Moffatt & Sellier 2002) as well as sophisticated boundary integral methods (Sellier 2003*b*). Other investigations have focused upon obtaining analytic solutions for idealized particle geometries in unbounded space. For example, the flow about a tri-axial ellipsoid was calculated by Sellier (2003*a*) and that about axisymmetric slender bodies was asymptotically analysed by Yariv & Miloh (2007).

† Email address for correspondence: yarive@technion.ac.il

https://doi.org/10.1017/S0022112008005193 Published online by Cambridge University Press

Since all practical devices are bounded in one or more dimensions, it is important to extend the preceding work by incorporating wall effects. The two simplest bounded configurations were described by Sellier (2005): the first consists of a spherical particle in the vicinity of a plane dielectric wall, where at large distances from the particle a uniform electric current is directed parallel to the wall. The second involves a conducting wall, the applied field being perpendicular to it; it can describe particle motion in the vicinity of an electrode (Keh & Anderson 1985). In both configurations, it is natural to assume that the magnetic field is applied perpendicular to the current, as it would be in typical engineering applications. In the first configuration, it may still possess an arbitrary orientation relative to the wall.

Both problems are governed by a single geometric parameter λ, the ratio of particle radius to the particle-wall distance. For $\lambda = O(1)$, they can be solved using bi-polar coordinates, where both the particle and wall boundaries constitute equi-coordinate surfaces. The formulation in terms of these coordinates was provided by Sellier (2005), who also solved the second problem (Sellier 2006). The solution of the electrostatic and flow equations using bi-polar coordinates solutions appears in the form of eigenfunction expansions. Integration over the particle surface provides the quantities of physical interest, namely expressions for the hydrodynamic loads (force and torque) acting on it.

It is important to emphasize that these quantities appear in the form of infinite converging series, whose coefficients must be determined by matrix inversion using truncation methods. Accordingly, they do not provide closed-form functional description for the behaviour of these loads as a function of the particle–wall separation (or, equivalently, of λ). It is therefore desired to supplement the bi-polar calculations with complementary asymptotic approximations for both small ($1-\lambda \ll 1$) and large ($\lambda \ll 1$) separations. This approach is common in various analyses of particle–particle and particle–wall interactions, including potential problems (Jeffery 1912; Bentwich & Miloh 1978; Solomentsev, Velegol & Anderson 1997), Stokes flows (Stimson & Jeffery 1926; Brenner 1961; O'Neill 1964; Goldman, Cox & Brenner 1967) and electrokinetics (Keh & Anderson 1985; Keh & Chen 1989; Yariv & Brenner 2003). The large-separation problems are handled via reflection methods, using the unbounded-fluid-domain solution (in the absence of a wall) as a first approximation; the small-separation problems are handled by appropriate lubrication approximations. In this paper we follow a similar approach and analyse the large-separation limit $\lambda \ll 1$.

We focus upon the first bounded configuration of Sellier (2005): the effect of a remote insulating wall upon the electro-magneto-phoretic motion of an insulating spherical particle. Such an insulating boundary constitutes a standard model for dielectric walls which are abundant in micro-channel experiments (Watarai *et al.* 2004). In principle, it is possible to extend the present analysis so as to handle conducting particles and walls. Note, however, that the common practice of modelling conducting surfaces using current-continuity boundary conditions (Leenov & Kolin 1954) is somewhat oversimplified as it does not account for the surface kinetics.

Since our interest is in assessing the wall effect, we adopt a relatively simple model, assuming the particle to possess the same magnetic permeability as that of the suspending liquid. The magnetic field is then uniform in the entire fluid domain. As is common in electro-magneto-phoretic analyses we take both the Reynolds and magnetic Reynolds numbers to be zero. Moreover, following Moffatt & Sellier (2002), we assume a vanishingly small Hartmann number. This assumption leads to two

https://doi.org/10.1017/S0022112008005193 Published online by Cambridge University Press

simplifications in the problem formulation: the electrostatic problem is uncoupled from the flow, and all flow variables are bilinear in the imposed electric and magnetic fields. This bilinearity enables us to analyse separately the cases of a magnetic field which is parallel to the wall, and one which is perpendicular to it. Due to the linearity of the Stokes equations in the velocity field, it is sufficient to analyse a stationary particle: Once the hydrodynamic loads on such a particle are evaluated, existing mobility relations (Happel & Brenner 1965; Kim & Karrila 1991) are utilized so as to provide the velocity of a freely suspended particle through the physical space.

The effect of a remote wall is studied using reflection techniques about the unbounded-fluid-domain solution of Leenov & Kolin (1954). The electric potential is obtained in the form of successive solutions that alternately satisfy the boundary conditions on either the particle or the wall. The evaluation of the velocity field is more complicated: in addition to the need to impose the zero-velocity condition on both surfaces, it is also necessary to account for the Lorentz body force associated with the preceding electric-potential reflections. Additional complications arise in transforming the velocity field of Leenov & Kolin (1954) to a Cartesian coordinate system aligned with the wall: since that field does not satisfy the homogeneous Stokes equations, the well-known Fourier representations of Faxén (Happel & Brenner 1965; Kim & Karrila 1991) are inadequate for that task.

The paper is organized as follows: In the next section, we formulate the governing equations and employ the symmetry arguments of Moffatt & Sellier (2002) to deduce the tensorial structure of the hydrodynamic loads. The large-separation iterative scheme is described in § 3. Section 4 is concerned with the evaluation of the leading-order corrections to the hydrodynamic reactions and the subsequent calculation of the rectilinear and angular velocities acquired by a freely suspended particle. Conclusions are drawn in § 5.

2. Problem formulation

An insulating spherical particle of radius a is positioned within a conducting liquid of matching magnetic permeability at distance a/λ ($\lambda < 1$) from a plane dielectric wall. The Newtonian liquid possesses a dynamic viscosity η and an electrical conductivity σ. The fluid domain is denoted by $\mathscr{D}$, the liquid–particle interface by $\mathscr{P}$ and the liquid–wall interface by $\mathscr{W}$. This system is exposed to a uniformly applied electric field $\boldsymbol{E} = E\hat{\boldsymbol{E}}$, where $\hat{\boldsymbol{E}}$ is a unit vector directed parallel to the wall, and a uniformly applied magnetic field $\boldsymbol{B} = B\hat{\boldsymbol{B}}$, where $\hat{\boldsymbol{B}}$ is a unit vector which is perpendicular to $\hat{\boldsymbol{E}}$. Our interest lies in the resulting hydrodynamic force and torque exerted on the particle.

We employ a dimensionless notation where length variables are scaled with a, the electric field with E and the electrical potential with aE. The corresponding scales for stresses, forces and torques are then respectively provided by σEBa, σEBa^3 and σEBa^4. The velocity field is normalized with $\sigma EBa^2/\eta$. We refer to the coordinate normalization with a as the 'inner description'.

It is convenient to define a Cartesian coordinate system $\boldsymbol{r} = (x, y, z)$ with the particle centre at its origin, the x-axis along the applied electric field and the z-axis perpendicular to wall. Thus, $\mathscr{W}$ is given by $z = -1/\lambda$ and $\hat{\boldsymbol{E}} = \hat{\boldsymbol{e}}_x$. It is also convenient to employ the spherical coordinates r and θ (see figure 1), $r = 0$ corresponding to the particle centre and the polar angle θ measured from the x-axis.

https://doi.org/10.1017/S0022112008005193 Published online by Cambridge University Press

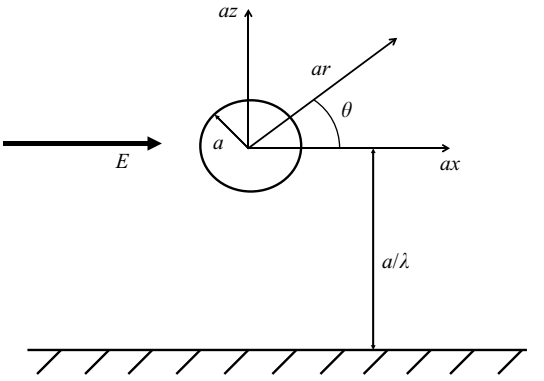


FIGURE 1. A schematic illustration of the particle–wall configuration.

2.1. *Governing equations*

The presence of the insulating particle modifies the electric field from its undisturbed value $\hat{\boldsymbol{E}}$ to $\hat{\boldsymbol{E}} - \nabla\varphi$. The liquid acts as an Ohmic conductor, with the current density being proportional to that field. Thus, charge conservation implies that the potential disturbance φ is governed by Laplace's equation

$$\nabla^2\varphi = 0 \quad \text{in} \quad \mathscr{D}; \tag{2.1}$$

also, the requirement that the solid surfaces are impermeable to electric current implies the Neumann-type boundary condition on the particle

$$\frac{\partial\varphi}{\partial r} = \cos\theta \quad \text{for} \quad r = 1 \tag{2.2}$$

and on the wall

$$\frac{\partial\varphi}{\partial z} = 0 \quad \text{for} \quad z = -1/\lambda; \tag{2.3}$$

additionally, φ is required to attenuate at large distances from the particle.

The applied fields result in the Lorentz force density distribution

$$\hat{\boldsymbol{E}} \times \hat{\boldsymbol{B}} - \nabla\varphi \times \hat{\boldsymbol{B}}. \tag{2.4}$$

The first term in (2.4) represents a uniform body force; it is balanced by a 'hydrostatic' pressure distribution, which in turn results in the electromagnetic buoyancy force

$$-\frac{4\pi}{3}\,\hat{\boldsymbol{E}} \times \hat{\boldsymbol{B}}. \tag{2.5}$$

The second term in (2.4) is rotational and cannot be balanced by any pressure distribution; thus, it results in a fluid motion. This motion is governed by the continuity equation

$$\nabla \cdot \boldsymbol{v} = 0 \tag{2.6}$$

and the inhomogeneous Stokes equation

$$\nabla^2\boldsymbol{v} = \nabla p + \nabla\varphi \times \hat{\boldsymbol{B}}. \tag{2.7}$$

Here, $\boldsymbol{v}$ is the velocity field and p is the 'modified' pressure, above and beyond the 'hydrostatic' distribution which generates (2.5). These equations are supplemented by the impermeability and no-slip boundary conditions on $\mathscr{W}$ and $\mathscr{P}$:

$$\boldsymbol{v} = \boldsymbol{0} \quad \text{for} \quad r = 1, \quad z = -1/\lambda, \tag{2.8}$$

https://doi.org/10.1017/S0022112008005193 Published online by Cambridge University Press

together with the requirement that $\boldsymbol{v}$ decays to zero at large distances away from the particle.

In what follows we consider two separate cases; one where $\hat{\boldsymbol{B}}$ lies normal to the wall (the 'perpendicular case') and the other where it lies parallel to it (the 'parallel case'). Because the governing equations are linear and homogeneous in $\hat{\boldsymbol{B}}$, the solution to the general situation of a magnetic field at an arbitrary angle to the wall can be retrieved via an appropriate superposition of the results corresponding to these two cases.

2.2. *Tensorial symmetry arguments*

As explained by Moffatt & Sellier (2002), the hydrodynamic force ($\boldsymbol{F}$) and torque ($\boldsymbol{G}$) animated by the applied fields are bilinear in the fixed vectors $\hat{\boldsymbol{E}}$ and $\hat{\boldsymbol{B}}$ and are therefore provided by the contractions

$$\boldsymbol{F} = \boldsymbol{\mathsf{F}} : \hat{\boldsymbol{E}}\,\hat{\boldsymbol{B}}, \quad \boldsymbol{G} = \boldsymbol{\mathsf{G}} : \hat{\boldsymbol{E}}\,\hat{\boldsymbol{B}}, \tag{2.9}$$

where $\boldsymbol{\mathsf{F}}$ is a third-order pseudo-tensor and $\boldsymbol{\mathsf{G}}$ is third-order true tensor. We employ the Gibbs convention for tensor contraction.

Since the bilinear dependence upon the applied fields has been factored out, the dimensionless coefficients $\boldsymbol{\mathsf{F}}$ and $\boldsymbol{\mathsf{G}}$ are purely geometric quantities, which depend only upon the particle–wall geometry. The only vector appearing in the specification of this geometry is the normal to the wall. Thus, the only possible candidates for $\boldsymbol{\mathsf{F}}$ are the isotropic pseudo-tensor $\boldsymbol{\epsilon}$, as well as $\boldsymbol{\epsilon}\cdot\hat{\boldsymbol{n}}\hat{\boldsymbol{n}}$ (and permutations thereof), where $\hat{\boldsymbol{n}}(=\hat{\boldsymbol{e}}_z)$ is a unit normal to the wall. It is readily found that if $\hat{\boldsymbol{B}}=\hat{\boldsymbol{e}}_y$ the force acts in the z-direction; if $\hat{\boldsymbol{B}}=\hat{\boldsymbol{e}}_z$ it acts in the y-direction.

There are no isotropic third-order true tensors, whence the only candidates for $\boldsymbol{\mathsf{G}}$ are $\hat{\boldsymbol{n}}\hat{\boldsymbol{n}}\hat{\boldsymbol{n}}$ and various permutations of $\boldsymbol{I}\hat{\boldsymbol{n}}$, $\boldsymbol{I}$ being the unit tensor. It is readily found that if $\hat{\boldsymbol{B}}=\hat{\boldsymbol{e}}_z$ the torque acts in the x-direction, while if $\hat{\boldsymbol{B}}=\hat{\boldsymbol{e}}_y$ the torque vanishes.

Similar tensorial arguments actually show that the case of parallel magnetic and electric fields (say $\hat{\boldsymbol{B}}=\hat{\boldsymbol{e}}_x$) is of no practical interest. For that case, it is already known (Moffatt & Sellier 2002) that the particle does not experience any loads when placed in an unbounded fluid domain. The presence of a nearby wall introduces new candidates for $\boldsymbol{\mathsf{F}}$, namely, $\boldsymbol{\epsilon}\cdot\hat{\boldsymbol{n}}\hat{\boldsymbol{n}}$ and permutations thereof. These candidates, however, vanish upon contraction with $\hat{\boldsymbol{e}}_x\hat{\boldsymbol{e}}_x$. The only effect generated by the wall is associated with the new candidate for $\boldsymbol{\mathsf{G}}$, $\hat{\boldsymbol{n}}\boldsymbol{I}$. This candidate results in a couple along the z-axis. Due to symmetry, this couple does not provoke any rectilinear particle motion.

3. Large separation analysis

We focus here upon the case where the particle–wall separation is large compared with the particle size, i.e. $\lambda \ll 1$. This allows for an iterative solution using a reflection scheme of the kind used in other classes of field-driven flows (Keh & Anderson 1985). The scheme consists of generating successive approximations that alternately satisfy the boundary conditions on either $\mathscr{P}$ or $\mathscr{W}$. The first approximation corresponds to a particle in an unbounded fluid domain ($\lambda \to 0$).

The electrostatic problem has already been solved in that manner by Keh & Anderson (1985) in a different physical context. Thus, the potential is provided by the iterative series

$$\varphi = \varphi^{(0)}_{\mathscr{P}} + \left[\varphi^{(1)}_{\mathscr{W}} + \varphi^{(1)}_{\mathscr{P}}\right] + \left[\varphi^{(2)}_{\mathscr{W}} + \varphi^{(2)}_{\mathscr{P}}\right] + \cdots \tag{3.1}$$

https://doi.org/10.1017/S0022112008005193 Published online by Cambridge University Press

wherein the first approximation is a dipole

$$\varphi^{(0)}_{\mathscr{P}} = -\frac{\cos\theta}{2r^2} = -\frac{x}{2[x^2+y^2+z^2]^{3/2}}. \tag{3.2}$$

The harmonic 'wall correction' $\varphi^{(n)}_{\mathscr{W}}$ $(n \geqslant 1)$ satisfies

$$\frac{\partial \varphi^{(n)}_{\mathscr{W}}}{\partial z} = -\frac{\partial \varphi^{(n-1)}_{\mathscr{P}}}{\partial z} \quad \text{for} \quad z = -1/\lambda, \tag{3.3}$$

in accordance with the no-flux condition (2.3) on the wall. Similarly, the harmonic 'particle correction' $\varphi^{(n)}_{\mathscr{P}}$ $(n \geqslant 1)$ satisfies

$$\frac{\partial \varphi^{(n)}_{\mathscr{P}}}{\partial r} = -\frac{\partial \varphi^{(n)}_{\mathscr{W}}}{\partial r} \quad \text{for} \quad r = 1, \tag{3.4}$$

in accordance with the no-flux condition (2.2) on the particle. Both fields are required to decay at large distances from the particle.

Consider now the flow field. The zeroth-order approximation $(\boldsymbol{v}^{(0)}_{\mathscr{P}}, p^{(0)}_{\mathscr{P}})$, corresponding to $\lambda \to 0$, was derived by Leenov & Kolin (1954). If $\hat{\boldsymbol{B}} = \hat{\boldsymbol{e}}_z$ their notation agrees with the present one. Thus,

$$\boldsymbol{v}^{(0)}_{\mathscr{P}} = \frac{1}{8}\left(\frac{1}{r^5} - \frac{1}{r^3}\right)[xy\hat{\boldsymbol{e}}_x + (z^2 - x^2)\hat{\boldsymbol{e}}_y - yz\hat{\boldsymbol{e}}_z]. \tag{3.5}$$

The velocity field for the case $\hat{\boldsymbol{B}} = \hat{\boldsymbol{e}}_y$ is obtained by simultaneously applying the transformations $z \to y$, $y \to -z$ to (3.5).

We present the iterative series (together with a similar one for p):

$$\boldsymbol{v} = \boldsymbol{v}^{(0)}_{\mathscr{P}} + \left[\boldsymbol{v}^{(1)}_{\mathscr{W}} + \boldsymbol{v}^{(1)}_{\mathscr{P}} + \boldsymbol{v}^{(1)}_{\varphi}\right] + \left[\boldsymbol{v}^{(2)}_{\mathscr{W}} + \boldsymbol{v}^{(2)}_{\mathscr{P}} + \boldsymbol{v}^{(2)}_{\varphi}\right] + \cdots, \tag{3.6}$$

in which all fields decay to zero at large distances from the particle. The pair $(\boldsymbol{v}^{(n)}_{\mathscr{W}}, p^{(n)}_{\mathscr{W}})$ $(n \geqslant 1)$ satisfies the homogeneous Stokes equations and the boundary condition

$$\boldsymbol{v}^{(n)}_{\mathscr{W}} = -\boldsymbol{v}^{(n-1)}_{\mathscr{P}} \quad \text{for} \quad z = -1/\lambda, \tag{3.7}$$

which restores the null value of $\boldsymbol{v}$ on $\mathscr{W}$ that is violated by $\boldsymbol{v}^{(n-1)}_{\mathscr{P}}$. Similarly, the pair $(\boldsymbol{v}^{(n)}_{\mathscr{P}}, p^{(n)}_{\mathscr{P}})$ $(n \geqslant 1)$ satisfies the homogeneous Stokes equations and the boundary condition

$$\boldsymbol{v}^{(n)}_{\mathscr{P}} = -\boldsymbol{v}^{(n)}_{\mathscr{W}} \quad \text{for} \quad r = 1, \tag{3.8}$$

which guarantees the null value of $\boldsymbol{v}$ on $\mathscr{P}$, which is violated by $\boldsymbol{v}^{(n)}_{\mathscr{W}}$.

In addition to the 'standard' reflections $\boldsymbol{v}^{(n)}_{\mathscr{W}}$ and $\boldsymbol{v}^{(n)}_{\mathscr{P}}$, it is also necessary to add proper corrections which handle the additional Lorentz terms which are engendered by the electric-potential reflections. Thus, the velocity field $\boldsymbol{v}^{(n)}_{\varphi}$ satisfies the inhomogeneous Stokes equation [cf. (2.7)]:

$$\nabla^2 \boldsymbol{v}^{(n)}_{\varphi} = \nabla p^{(n)}_{\varphi} + \nabla\left(\varphi^{(n)}_{\mathscr{W}} + \varphi^{(n)}_{\mathscr{P}}\right) \times \hat{\boldsymbol{B}}, \tag{3.9}$$

and vanishes on both $\mathscr{P}$ and $\mathscr{W}$. This field restores the momentum balance which is violated by the body force associated with the electric-potential corrections.

Note that the wall reflections do not directly contribute to the hydrodynamic load, since they are regular within the particle. Moreover, the contribution $\boldsymbol{F}^{(n)}_{\mathscr{P}}$ and $\boldsymbol{G}^{(n)}_{\mathscr{P}}$ arising from particle reflection $n(\geqslant 1)$ are simply provided by Faxén's laws (Happel & Brenner 1965) applied upon the predecessor wall reflection which

https://doi.org/10.1017/S0022112008005193 Published online by Cambridge University Press

'triggered' it:

$$\boldsymbol{F}^{(n)}_{\mathscr{P}} = \left[6\pi \boldsymbol{v}^{(n)}_{\mathscr{W}} + \pi\nabla^2 \boldsymbol{v}^{(n)}_{\mathscr{W}}\right]_{r=0}, \quad \boldsymbol{G}^{(n)}_{\mathscr{P}} = 4\pi\left[\nabla \times \boldsymbol{v}^{(n)}_{\mathscr{W}}\right]_{r=0}. \tag{3.10}$$

4. Leading-order correction

The loads exerted in an unbounded domain, resulting from the zeroth-order flow field $\boldsymbol{v}^{(0)}_{\mathscr{P}}$, were already calculated by Leenov & Kolin (1954):

$$\boldsymbol{F}^{(0)} = \frac{\pi}{3}\hat{\boldsymbol{E}} \times \hat{\boldsymbol{B}}, \quad \boldsymbol{G}^{(0)} = \boldsymbol{0}. \tag{4.1}$$

Our interest lies in the wall-induced leading-order correction to (4.1). Towards this end, it is sufficient to evaluate the loads delivered by the leading-order flow corrections.

The contribution of $\boldsymbol{v}^{(1)}_{\varphi}$ is relatively easy to find, since the first few terms in (3.1) have already been determined by Keh & Anderson (1985). Thus, $\varphi^{(1)}_{\mathscr{W}}$ represents a mirror dipole positioned at $z = -2/\lambda$:

$$\varphi^{(1)}_{\mathscr{W}} = -\frac{x}{2[x^2 + y^2 + (z + 2/\lambda)^2]^{3/2}}. \tag{4.2}$$

Taylor expansion near the particle centre yields

$$\varphi^{(1)}_{\mathscr{W}} \sim -\frac{x\lambda^3}{16}\left[1 + O(\lambda)\right]. \tag{4.3}$$

The leading term in this expression represents a uniform electric field in the x-direction of magnitude $\lambda^3/16$. The effect of a uniform field is already known from the solution of Leenov & Kolin (1954) (cf. (2.5) and (4.1)), whence

$$\boldsymbol{F}^{(1)}_{\varphi} = -\frac{\pi}{16}\lambda^3\, \hat{\boldsymbol{E}} \times \hat{\boldsymbol{B}} + O(\lambda^4), \quad \boldsymbol{G}^{(1)}_{\varphi} = O(\lambda^4). \tag{4.4}$$

To evaluate the loads delivered by $\boldsymbol{v}^{(1)}_{\mathscr{P}}$ we need to calculate $\boldsymbol{v}^{(1)}_{\mathscr{W}}$ and then apply Faxén's relations (3.10) for $n = 1$.

4.1. *The first wall reflection*

To evaluate $\boldsymbol{v}^{(1)}_{\mathscr{W}}$ it is convenient to follow Ho & Leal (1974) and employ an 'outer' description $\boldsymbol{R} = (X, Y, Z)$ defined by $\boldsymbol{R} = \lambda \boldsymbol{r}$:

$$X = \lambda x, \quad Y = \lambda y, \quad Z = \lambda z, \quad R = \lambda r, \quad \nabla = \lambda \nabla_{\boldsymbol{R}}. \tag{4.5}$$

Expressed in the outer variables, $\mathscr{W}$ is the plane $Z = -1$ and $\mathscr{P}$ is the sphere $R = \lambda$. When using outer variables $\boldsymbol{v}^{(0)}_{\mathscr{P}}$ is $O(\lambda)$. This reflects the $1/r$ decay rate in (3.5).

Since $\boldsymbol{v}^{(1)}_{\mathscr{W}}$ satisfies the homogeneous Stokes equations, it can be expressed using Faxén's Fourier integral representation (Happel & Brenner 1965). Following Ho & Leal (1974) we express the Cartesian components of $\boldsymbol{v}^{(1)}_{\mathscr{W}}$ in the form:

$$\left.\begin{aligned} u^{(1)}_{\mathscr{W}} &= \mathscr{F}\left\{\left[g_1 + \frac{\alpha^2}{k^2}(g_2 + kZg_3)\right]\mathrm{e}^{-kZ}\right\}, \\ v^{(1)}_{\mathscr{W}} &= \mathscr{F}\left\{\frac{\alpha\beta}{k^2}\left[g_2 + kZg_3\right]\mathrm{e}^{-kZ}\right\}, \\ w^{(1)}_{\mathscr{W}} &= \mathscr{F}\left\{\frac{\mathrm{i}\alpha}{k}\left[g_1 + g_2 + g_3(1 + kZ)\right]\mathrm{e}^{-kZ}\right\}, \end{aligned}\right\} \tag{4.6}$$

https://doi.org/10.1017/S0022112008005193 Published online by Cambridge University Press

wherein $k=(\alpha^2+\beta^2)^{1/2}$ and g_1, g_2 and g_3 are arbitrary functions of α and β. Here, $\mathscr{F}$ denotes a two-dimensional Fourier transform, defined generically by

$$\mathscr{F}\{f\}=\frac{1}{2\pi}\int_{-\infty}^{\infty}\int_{-\infty}^{\infty}f(\alpha,\beta)\,\mathrm{e}^{\mathrm{i}(\alpha X+\beta Y)}\,\mathrm{d}\alpha\,\mathrm{d}\beta. \tag{4.7}$$

Towards application of (3.10), we use (4.5) and (4.6) to obtain

$$\left.\begin{aligned}
\left[\boldsymbol{v}^{(1)}_{\mathscr{W}}\right]_{r=0}&=\mathscr{F}\left\{\left(g_1+\frac{\alpha^2}{k^2}g_2\right)\hat{\boldsymbol{e}}_x+\frac{\alpha\beta}{k^2}g_2\hat{\boldsymbol{e}}_y+\frac{\mathrm{i}\alpha}{k}(g_1+g_2+g_3)\hat{\boldsymbol{e}}_z\right\},\\
\left[\nabla^2\boldsymbol{v}^{(1)}_{\mathscr{W}}\right]_{r=0}&=-2\lambda^2\mathscr{F}\left\{\alpha^2 g_3\hat{\boldsymbol{e}}_x+\alpha\beta g_3\hat{\boldsymbol{e}}_y+\mathrm{i}\alpha k g_3\hat{\boldsymbol{e}}_z\right\},\\
\left[\nabla\times\boldsymbol{v}^{(1)}_{\mathscr{W}}\right]_{r=0}&=\lambda\mathscr{F}\left\{-\frac{\alpha\beta}{k}(g_1+2g_3)\hat{\boldsymbol{e}}_x+\frac{2\alpha^2 g_3-\beta^2 g_1}{k}\hat{\boldsymbol{e}}_y-\mathrm{i}\beta g_1\hat{\boldsymbol{e}}_z\right\}.
\end{aligned}\right\} \tag{4.8}$$

The functions g_1, g_2 and g_3 are determined by imposing (3.7) for $n=1$. Thus, it is first required to represent $\boldsymbol{v}^{(0)}_{\mathscr{P}}$ as a Fourier integral. This requirement is familiar from previous applications of Faxén's Fourier representation (Ho & Leal 1974; Magnaudet, Takagi & Legendre 2003); in the present case, however, it introduces some difficulties, since $\boldsymbol{v}^{(0)}_{\mathscr{P}}$ is not a solution of the homogeneous Stokes equations and thus cannot be expressed in a form similar to (4.6). It is therefore necessary to represent the following expressions (cf. (3.5)):

$$\frac{1}{R^3},\quad\frac{X}{R^3},\quad\frac{Y}{R^3},\quad\frac{XY}{R^3},\quad\frac{X^2}{R^3},\quad\frac{Y^2}{R^3},\quad\frac{1}{R^5},\quad\frac{X}{R^5},\quad\frac{Y}{R^5},\quad\frac{X^2}{R^5},\quad\frac{Y^2}{R^5},\quad\frac{XY}{R^5} \tag{4.9}$$

as Fourier integrals (evaluated at $Z=-1$). This is done in Appendix A.

Imposing (3.7) for $n=1$ then provides the requisite expressions for g_1, g_2 and g_3 (see Appendix B). Note that these expressions are pre-factored by λ; indeed, since $\boldsymbol{v}^{(0)}_{\mathscr{P}}$ is $O(\lambda)$ in the outer scale, then so must also be $\boldsymbol{v}^{(1)}_{\mathscr{W}}$.

4.2. *The hydrodynamic loads*

Substituting the expressions for g_1, g_2 and g_3 into (4.8), performing the integration over the (α,β) plane using polar coordinates and using (3.10) yields the force and torque triggered by $\boldsymbol{v}^{(1)}_{\mathscr{W}}$. For $\hat{\boldsymbol{B}}=\hat{\boldsymbol{e}}_z$ we employ (B 1) to obtain

$$\boldsymbol{F}^{(1)}_{\mathscr{P}}=\frac{\pi}{16}\lambda^3\hat{\boldsymbol{e}}_y+O(\lambda^5),\quad \boldsymbol{G}^{(1)}_{\mathscr{P}}=\frac{\pi}{4}\lambda^2\hat{\boldsymbol{e}}_x+O(\lambda^4). \tag{4.10}$$

The directions of these hydrodynamic loads agree with the tensorial requirements. Employing (B 2) for the case $\hat{\boldsymbol{B}}=\hat{\boldsymbol{e}}_y$ yields zero force and torque. The absence of a torque in that case is also in accordance with the tensorial requirements.

Since at the outer scale $\boldsymbol{v}^{(1)}_{\mathscr{W}}$ is $O(\lambda)$ one may expect a leading $O(\lambda)$ contribution to $\boldsymbol{F}^{(1)}_{\mathscr{P}}$ from the first term in (3.10). However, the explicit calculation shows that $\boldsymbol{v}^{(1)}_{\mathscr{W}}$ actually vanishes at $r=0$, whence the leading $O(\lambda^3)$ contribution to $\boldsymbol{F}^{(1)}_{\mathscr{P}}$ arises from the Laplacian of $\boldsymbol{v}^{(1)}_{\mathscr{W}}$. To verify that a leading-order correction has indeed been attained, it is therefore necessary to inspect the leading-order contribution to the force which is triggered by $\boldsymbol{v}^{(2)}_{\mathscr{W}}$. Expanding $\boldsymbol{v}^{(1)}_{\mathscr{W}}$ into a Taylor series about $\boldsymbol{R}=\boldsymbol{0}$ yields

$$\boldsymbol{v}^{(1)}_{\mathscr{W}}=\left[\boldsymbol{v}^{(1)}_{\mathscr{W}}\right]_{\boldsymbol{R}=\boldsymbol{0}}+\boldsymbol{R}\cdot\left[\nabla_{\boldsymbol{R}}\boldsymbol{v}^{(1)}_{\mathscr{W}}\right]_{\boldsymbol{R}=\boldsymbol{0}}+\tfrac{1}{2}\boldsymbol{R}\boldsymbol{R}:\left[\nabla_{\boldsymbol{R}}\nabla_{\boldsymbol{R}}\boldsymbol{v}^{(1)}_{\mathscr{W}}\right]_{\boldsymbol{R}=\boldsymbol{0}}+\cdots. \tag{4.11}$$

Since $\boldsymbol{v}^{(1)}_{\mathscr{W}}$ is $O(\lambda)$, then so are its gradients with respect to outer coordinates. When transforming to inner coordinates towards application of (3.8) with $n=1$, (4.11)

https://doi.org/10.1017/S0022112008005193 Published online by Cambridge University Press

becomes an asymptotic sequence in powers of λ. Since $\boldsymbol{v}^{(1)}_{\mathscr{W}}$ was found to vanish at $\boldsymbol{R}=\boldsymbol{0}$, the leading $O(\lambda^2)$ contribution to (4.11) arises from the second term there, and is linear in $\boldsymbol{r}$. Accordingly, $\boldsymbol{v}^{(1)}_{\mathscr{P}}$ is $O(\lambda^2)$ when expressed in inner coordinates. When rewriting $\boldsymbol{v}^{(1)}_{\mathscr{P}}$ in outer variables, its order of magnitude depends upon its decay rate, a $1/r^n$ rate resulting in a λ^n multiplicative factor. Since an ambient velocity term which is linear in $\boldsymbol{r}$ is known to result in a velocity disturbance that decays as $1/r^2$ (Leal 1992), $\boldsymbol{v}^{(1)}_{\mathscr{P}}$ is $O(\lambda^4)$ at the outer description and whence so must be $\boldsymbol{v}^{(2)}_{\mathscr{W}}$. According to (3.10) and (4.5), the force and torque triggered by $\boldsymbol{v}^{(2)}_{\mathscr{W}}$ are at most $O(\lambda^4)$ and $O(\lambda^5)$, respectively.

Combining (2.5), (4.1), (4.4) and (4.10), and taking into account the symmetry arguments of § 2.2, we therefore find that the perpendicular case $\hat{\boldsymbol{B}}=\hat{\boldsymbol{e}}_z$ results in the loads

$$\boldsymbol{F}=\pi\left[1+\frac{1}{8}\lambda^3+O(\lambda^4)\right]\hat{\boldsymbol{e}}_y,\quad \boldsymbol{G}=\left[\frac{\pi}{4}\lambda^2+O(\lambda^4)\right]\hat{\boldsymbol{e}}_x, \tag{4.12}$$

while the parallel case $\hat{\boldsymbol{B}}=\hat{\boldsymbol{e}}_y$ results in the force

$$\boldsymbol{F}=-\pi\left[1+\tfrac{1}{16}\lambda^3+O(\lambda^4)\right]\hat{\boldsymbol{e}}_z. \tag{4.13}$$

and in a zero torque.

4.3. *The velocity of a freely suspended particle*

If the particle is freely suspended, its translational velocity $\boldsymbol{U}$ and angular velocity $\boldsymbol{\Omega}$ due to the loads $\boldsymbol{F}$ and $\boldsymbol{G}$ are obtained by employing the mobility relations (Happel & Brenner 1965; Kim & Karrila 1991):

$$\boldsymbol{U}=\boldsymbol{M}\cdot\boldsymbol{F}+\boldsymbol{C}\cdot\boldsymbol{G},\quad \boldsymbol{\Omega}=\boldsymbol{C}^{\dagger}\cdot\boldsymbol{F}+\boldsymbol{N}\cdot\boldsymbol{G}. \tag{4.14}$$

Here, the dimensionless tensorial coefficients $\boldsymbol{M}$, $\boldsymbol{C}$ and $\boldsymbol{N}$ are functions of the particle–wall geometry. Thus, the true tensor $\boldsymbol{M}$ possesses the transversally symmetric forms

$$\boldsymbol{M}=(\boldsymbol{I}-\hat{\boldsymbol{n}}\hat{\boldsymbol{n}})M^{\parallel}(\lambda)+\hat{\boldsymbol{n}}\hat{\boldsymbol{n}}M^{\perp}(\lambda) \tag{4.15}$$

(as does the true tensor $\boldsymbol{N}$), whereas the pseudo-tensor $\boldsymbol{C}$ is given by $\boldsymbol{\epsilon}\cdot\hat{\boldsymbol{n}}\,C(\lambda)$.

The scalar coefficients appearing in these expressions have already been calculated for $\lambda\ll 1$ (Happel & Brenner 1965; Kim & Karrila 1991):

$$6\pi M^{\parallel}(\lambda)=1-\tfrac{9}{16}\lambda+\tfrac{1}{8}\lambda^3+O(\lambda^4),\quad 6\pi M^{\perp}(\lambda)=1-\tfrac{9}{8}\lambda+\tfrac{1}{2}\lambda^3+O(\lambda^4), \tag{4.16}$$

$$64\pi C(\lambda)=\lambda^4+O(\lambda^5). \tag{4.17}$$

We are not familiar with any evaluation of $\boldsymbol{N}$ for $\lambda\ll 1$; nevertheless, the known mobility relation (Leal 1992) for a particle which is suspended in an unbounded liquid domain,

$$\boldsymbol{N}(\lambda)\to\frac{1}{8\pi}\boldsymbol{I}\quad\text{as}\quad\lambda\to 0, \tag{4.18}$$

is sufficient for the present analysis. Using (4.12) and (4.13) we therefore find that the particle translational velocity for the perpendicular and parallel cases is respectively given by

$$\boldsymbol{U}=\tfrac{1}{6}\left[1-\tfrac{9}{16}\lambda+\tfrac{1}{4}\lambda^3+O(\lambda^4)\right]\hat{\boldsymbol{e}}_y,\quad \boldsymbol{U}=-\tfrac{1}{6}\left[1-\tfrac{9}{8}\lambda+\tfrac{9}{16}\lambda^3+O(\lambda^4)\right]\hat{\boldsymbol{e}}_z. \tag{4.19}$$

Since the torque is $O(\lambda^2)$ at most, it is clear from (4.17) that for $O(\lambda^3)$ this velocity is only affected by the force. For the perpendicular case the particle also acquires an angular velocity along the x-axis of magnitude $\lambda^2/32+O(\lambda^4)$.

https://doi.org/10.1017/S0022112008005193 Published online by Cambridge University Press

5. Concluding remarks

We have investigated the effect of a remote solid wall upon the hydrodynamic loads experienced by a spherical insulating particle which is exposed to an externally imposed uniform electric current, which lies parallel to the wall, and a perpendicular magnetic field, which is either parallel or perpendicular to the wall.

We have employed an iterative reflection scheme which provides asymptotic expansions for the hydrodynamic loads acting on the particle. Our interest resides in obtaining the leading-order corrections to the unbounded-fluid-domain loads. While the slow $1/r$ decay of the unbounded-fluid-domain velocity field suggests an $O(\lambda)$ force correction, it turns out that the force is actually $O(\lambda^3)$. This wall contribution enhances the unbounded-fluid-domain force. The magnitude of this enhancement for the perpendicular case is twice as large as that in the parallel case. The perpendicular case also results in an $O(\lambda^2)$ torque along the applied current.

When the magnetic field lies parallel to wall one can distinguish between two scenarios. If the magnetic field lies in the positive direction of $\hat{\boldsymbol{E}} \times \hat{\boldsymbol{n}}$, the particle is repelled from the wall. Otherwise, it is attracted to it, implying that the remote-wall approximation must eventually break down.

The weak long-range decay of the wall effect resembles that of typical electrophoretic phenomena (Keh & Anderson 1985). Electrophoretic motion, however, is force free; while no external forces act on the particle in the present mechanism, the well-known properties of force-free motion in the creeping-flow régime do not apply since the flow is not governed by the homogeneous Stokes equations.

Appendix A. Fourier integral representation of $\boldsymbol{v}_{\mathscr{P}}^{(1)}$

Our staring point is the representation (Happel & Brenner 1965)

$$\frac{1}{R} = \mathscr{F}\left\{\frac{\mathrm{e}^{-k|Z|}}{k}\right\} \tag{A 1}$$

where near $Z=-1$ we replace $|Z|$ by $-Z$. Upon using the relation

$$\frac{\partial}{\partial \xi}\left(\frac{1}{R}\right) = -\frac{\xi}{R^3}, \quad \xi = X, Y, Z, \tag{A 2}$$

and differentiating under the integral sign, we readily obtain

$$\frac{X}{R^3} = -\mathrm{i}\mathscr{F}\left\{\frac{\alpha \mathrm{e}^{kZ}}{k}\right\}, \quad \frac{Y}{R^3} = -\mathrm{i}\mathscr{F}\left\{\frac{\beta \mathrm{e}^{kZ}}{k}\right\}, \quad \frac{Z}{R^3} = -\mathscr{F}\{\mathrm{e}^{kZ}\}. \tag{A 3}$$

Specifically, substituting $Z=-1$ in the last expression yields

$$\left(\frac{1}{R^3}\right)_{Z=-1} = \mathscr{F}\{\mathrm{e}^{-k}\}. \tag{A 4}$$

Following that, we employ the relation

$$\frac{\xi}{R^5} = -\frac{1}{3}\frac{\partial}{\partial \xi}\left(\frac{1}{R^3}\right), \tag{A 5}$$

Using (A 4) for ξ being either X or Y and exploiting the commutativity in differentiating with respect to ξ and evaluation at $Z=-1$ we readily obtain

$$\left(\frac{X}{R^5}\right)_{Z=-1} = -\frac{\mathrm{i}}{3}\mathscr{F}\{\alpha \mathrm{e}^{-k}\}, \quad \left(\frac{Y}{R^5}\right)_{Z=-1} = -\frac{\mathrm{i}}{3}\mathscr{F}\{\beta \mathrm{e}^{-k}\}. \tag{A 6}$$

https://doi.org/10.1017/S0022112008005193 Published online by Cambridge University Press

Similarly, using the relation

$$\frac{\partial^2}{\partial \xi^2}\left(\frac{1}{R}\right) = 3\frac{\xi^2}{R^5} - \frac{1}{R^3}, \tag{A 7}$$

in conjunction with (A 1) and (A 4), yields

$$\left(\frac{X^2}{R^5}\right)_{Z=-1} = \frac{1}{3}\mathscr{F}\{\mathrm{e}^{-k}\} - \frac{1}{3}\mathscr{F}\{\alpha^2\mathrm{e}^{-k}\} \tag{A 8}$$

and

$$\left(\frac{Y^2}{R^5}\right)_{Z=-1} = \frac{1}{3}\mathscr{F}\{\mathrm{e}^{-k}\} - \frac{1}{3}\mathscr{F}\{\beta^2\mathrm{e}^{-k}\}. \tag{A 9}$$

Application of (A 7) for $\xi = Z$ at $Z = -1$ yields

$$\left(\frac{1}{R^5}\right)_{Z=-1} = \frac{1}{3}\mathscr{F}\{k\mathrm{e}^{-k}\} + \frac{1}{3}\mathscr{F}\{\mathrm{e}^{-k}\}. \tag{A 10}$$

The last expression found using this technique is XY/R^5; using the relation

$$\frac{\partial}{\partial X}\left(\frac{Y}{R^3}\right) = -3\frac{XY}{R^5} \tag{A 11}$$

and employing (A 6) yields

$$\frac{XY}{R^5} = -\frac{1}{3}\mathscr{F}\left\{\frac{\alpha\beta}{k}\mathrm{e}^{kZ}\right\}. \tag{A 12}$$

To obtain the remaining expressions in (4.9) we employ the inverse Fourier transformation for any function f of X and Y:

$$\mathscr{F}^{-1}\{f\} = \frac{1}{2\pi}\int_{-\infty}^{\infty}\int_{-\infty}^{\infty} f(X, Y)\,\mathrm{e}^{-\mathrm{i}(\alpha X+\beta Y)}\,\mathrm{d}X\,\mathrm{d}Y. \tag{A 13}$$

Differentiation under the integral provides the relations

$$\mathscr{F}^{-1}\left\{\frac{X^2}{R^3}\right\} = -\frac{\partial^2}{\partial\alpha^2}\mathscr{F}^{-1}\left\{\frac{1}{R^3}\right\}, \quad \mathscr{F}^{-1}\left\{\frac{Y^2}{R^3}\right\} = -\frac{\partial^2}{\partial\beta^2}\mathscr{F}^{-1}\left\{\frac{1}{R^3}\right\}, \tag{A 14}$$

which, upon use of (A 4), readily yield

$$\left(\frac{X^2}{R^3}\right)_{Z=-1} = \mathscr{F}\left\{\left(\frac{1}{k} - \frac{\alpha^2}{k^3} - \frac{\alpha^2}{k^2}\right)\mathrm{e}^{-k}\right\} \tag{A 15}$$

and

$$\left(\frac{Y^2}{R^3}\right)_{Z=-1} = \mathscr{F}\left\{\left(\frac{1}{k} - \frac{\beta^2}{k^3} - \frac{\beta^2}{k^2}\right)\mathrm{e}^{-k}\right\}. \tag{A 16}$$

Similarly, differentiation under the integral gives

$$\mathscr{F}^{-1}\left\{\frac{XY}{R^3}\right\} = \mathrm{i}\frac{\partial}{\partial\beta}\mathscr{F}^{-1}\left\{\frac{X}{R^3}\right\}, \tag{A 17}$$

which, using (A 6), results in

$$\frac{XY}{R^3} = -\mathscr{F}\left\{\frac{\alpha\beta}{k^3}(1 - kZ)\,\mathrm{e}^{kZ}\right\}. \tag{A 18}$$

https://doi.org/10.1017/S0022112008005193 Published online by Cambridge University Press

Appendix B. The functions g_1, g_2 and g_3

The functions g_1, g_2 and g_3 are calculated from the Fourier transform of (3.7) for $n=1$. In the perpendicular case we find

$$g_1 = \frac{\alpha\lambda e^{-2k}}{24\beta k^3}(\lambda^2k^4 - 3k^3 + \alpha^2\lambda^2k^2 + \beta^2\lambda^2k^2 + 3k^2 - 3\alpha^2k - 3\beta^2k - 3\alpha^2 - 3\beta^2), \quad (B\,1a)$$

$$g_2 = \frac{\lambda e^{-2k}}{24\alpha\beta k^2}(\lambda^2k^6 - \lambda^2k^5 - 3k^5 + \beta^2\lambda^2k^4 + 6k^4 - 3\beta^2k^3 - \alpha^2\lambda^2k^3 - 3k^3 - 3\alpha^2k^2 - \alpha^4\lambda^2k^2 - \alpha^2\beta^2\lambda^2k^2 + 3\alpha^4k + 3\alpha^2k + 3\alpha^2\beta^2k + 3\alpha^4 + 3\alpha^2\beta^2) \quad (B\,1b)$$

and

$$g_3 = \frac{\lambda e^{-2k}}{24\alpha\beta k^3}(\lambda^2k^6 - 3k^5 + \beta^2\lambda^2k^4 + 3k^4 - 3\beta^2k^3 - 6\alpha^2k^2 - \alpha^4\lambda^2k^2 - \alpha^2\beta^2\lambda^2k^2 + 3\alpha^4k + 3\alpha^2\beta^2k + 3\alpha^4 + 3\alpha^2\beta^2). \quad (B\,1c)$$

In the parallel case we find

$$g_1 = \frac{i\alpha\lambda e^{-2k}}{12k}(k\lambda^2 - 3), \quad (B\,2a)$$

$$g_2 = \frac{i\lambda e^{-2k}}{24\alpha k}(\lambda^2k^4 - \lambda^2k^3 - 3k^3 - 3\alpha^2\lambda^2k^2 + \beta^2\lambda^2k^2 + 3k^2 + 9\alpha^2k - 3\beta^2k + 3\alpha^2 - 3\beta^2) \quad (B\,2b)$$

and

$$g_3 = \frac{i\lambda e^{-2k}}{24\alpha k^2}(\lambda^2k^4 - 3k^3 - 3\alpha^2\lambda^2k^2 + \beta^2\lambda^2k^2 + 9\alpha^2k - 3\beta^2k + 3\alpha^2 - 3\beta^2). \quad (B\,2c)$$

REFERENCES

Bentwich, M. & Miloh, T. 1978 On the exact solution for the two-sphere problem in axisymmetric potential flow. *J. Appl. Mech.* **45**, 463–468.

Brenner, H. 1961 The slow motion of a sphere through a viscous fluid towards a plane surface. *Chem. Engng Sci.* **16**, 242–251.

Goldman, A. J., Cox, R. & Brenner, H. 1967 Slow viscous motion of a sphere parallel to a plane wall – I. Motion through a quiescent fluid. *Chem. Engng Sci.* **22**, 637–651.

Happel, J. & Brenner, H. 1965 *Low Reynolds Number Hydrodynamics*. Prentice-Hall.

Ho, B. P. & Leal, L. G. 1974 Inertial migration of rigid spheres in two-dimensional unidirectional flows. *J. Fluid Mech.* **65**, 365–400.

Jeffery, G. 1912 On a form of the solution of Laplace's equation suitable for problems relating to two spheres. *Proc. Roy. Soc. Lond.* A **87** (593), 109–120.

Keh, H. J. & Anderson, J. L. 1985 Boundary effects on electrophoretic motion of colloidal spheres. *J. Fluid Mech.* **153**, 417–439.

Keh, H. J. & Chen, S. B. 1989 Electrophoresis of a colloidal sphere parallel to a dielectric plane. *J. Fluid Mech.* **194**, 377–390.

Kim, S. & Karrila, S. J. 1991 *Microhydrodynamics*. Butterworth-Heinemann.

Kolin, A. 1978 Some current and potential uses of magnetic-fields in electrokinetic separations. *J. Chromatogr.* **159** (1), 147–181.

Kolin, A. & Kado, R. 1958 Fractionation of cell suspensions in an slectromagnetic force field. *Nature* **182** (4634), 510–512.

Leal, L. G. 1992 *Laminar Flow and Convective Transport Processes*. Butterworth-Heinemann.

Leenov, D. & Kolin, A. 1954 Theory of electromagnetophoresis. I. Magnetohydrodynamic forces experienced by spherical and symmetrically oriented cylindrical particles. *J. Chem. Phys.* **22** (4), 683–688.

https://doi.org/10.1017/S0022112008005193 Published online by Cambridge University Press

Magnaudet, J., Takagi, S. & Legendre, D. 2003 Drag, deformation and lateral migration of a buoyant drop moving near a wall. *J. Fluid Mech.* **476**, 115–157.

Moffatt, H. K. & Sellier, A. 2002 Migration of an insulating particle under the action of uniform ambient electric and magnetic fields. Part 1. General theory. *J. Fluid Mech.* **464**, 279–286.

O'Neill, M. E. 1964 A slow motion of a viscous liquid caused by a slowly moving solid sphere. *Mathematika* **11**, 64–74.

Sellier, A. 2003*a* Migration of a conducting ellipsoid subject to uniform ambient electric and magnetic fields. *C. R. Mécanique* **331** (2), 127–132.

Sellier, A. 2003*b* Migration of an insulating particle under the action of uniform ambient electric and magnetic fields. Part 2. Boundary formulation and ellipsoidal particles. *J. Fluid Mech.* **488**, 335–353.

Sellier, A. 2005 Migration of a solid conducting sphere immersed in a liquid metal near a plane boundary under the action of uniform ambient electric and magnetic fields. In *The 15th Riga and 6th PAMIR International Conference on Fundamental and Applied MHD*, pp. 311–314.

Sellier, A. 2006 Migration of a solid conducting sphere immersed in a liquid metal near a plane conducting solid wall under the action of uniform ambient electric and magnetic fields. *Magnetohydrodynamics* **42**, 317–326.

Solomentsev, Y., Velegol, D. & Anderson, J. L. 1997 Conduction in the small gap between two spheres. *Phys. Fluids* **9**, 1209–1217.

Stimson, M. & Jeffery, G. 1926 The motion of two spheres in a viscous fluid. *Proc. Roy. Soc.* A **111** (757), 110–116.

Watarai, H., Suwa, M. & Iiguni, Y. 2004 Magnetophoresis and electromagnetophoresis of microparticles in liquids. *Anal. Bioanal. Chem.* **378** (7), 1693–1699.

Xu, Z. M., Li, T. X. & Zhou, Y. H. 2007 Continuous removal of nonmetallic inclusions from aluminum melts by means of stationary electromagnetic field and dc current. *Metall. Mater. Trans.* A **38A**, 1104–1110.

Yariv, E. & Brenner, H. 2003 Near-contact electrophoretic motion of a sphere parallel to a planar wall. *J. Fluid Mech.* **484**, 85–111.

Yariv, E. & Miloh, T. 2007 Electro-magneto-phoresis of slender bodies. *J. Fluid Mech.* **577**, 331–340.

https://doi.org/10.1017/S0022112008005193 Published online by Cambridge University Press